


# Matrix approach to land carbon cycle modeling: A case study with the Community Land Model

Yuanyuan Huang<sup>1,2\*</sup>  | Xingjie Lu<sup>1,3\*</sup> | Zheng Shi<sup>1</sup> | David Lawrence<sup>4</sup> | Charles D. Koven<sup>5</sup> | Jianyang Xia<sup>6,7</sup> | Zhenggang Du<sup>7</sup> | Erik Kluzek<sup>4</sup> | Yiqi Luo<sup>1,3,8</sup>

<sup>1</sup>Department of Microbiology and Plant Biology, University of Oklahoma, Norman, OK, USA

<sup>2</sup>Now at Laboratoire des Sciences du Climat et de l'Environnement, Gif-sur-Yvette, France

<sup>3</sup>Center for Ecosystem Science and Society, Northern Arizona University, Flagstaff, AZ, USA

<sup>4</sup>Climate and Global Dynamics Division, National Center for Atmospheric Research, Boulder, CO, USA

<sup>5</sup>Earth Sciences Division, Lawrence Berkeley National Laboratory, Berkeley, CA, USA

<sup>6</sup>Tiantong National Forest Ecosystem Observation and Research Station, School of Ecological and Environmental Sciences, East China Normal University, Shanghai, China

<sup>7</sup>Research Center for Global Change and Ecological Forecasting, East China Normal University, Shanghai, China

<sup>8</sup>Department of Earth System Science, Tsinghua University, Beijing, China

## Correspondence

Yuanyuan Huang, Laboratoire des Sciences du Climat et de l'Environnement, Gif-sur-Yvette, France.

Email: [yuanyuanhuang2011@gmail.com](mailto:yuanyuanhuang2011@gmail.com)

Xingjie Lu, Center for Ecosystem Science and Society, Northern Arizona University, Flagstaff, AZ, USA.

Email: [Xingjie.Lu@nau.edu](mailto:Xingjie.Lu@nau.edu)

## Funding information

US Department of Energy, Grant/Award Number: DE-SC0008270, DE-SC00114085; US National Science Foundation (NSF), Grant/Award Number: EF 1137293, OIA-1301789

## Abstract

The terrestrial carbon (C) cycle has been commonly represented by a series of C balance equations to track C influxes into and effluxes out of individual pools in earth system models (ESMs). This representation matches our understanding of C cycle processes well but makes it difficult to track model behaviors. It is also computationally expensive, limiting the ability to conduct comprehensive parametric sensitivity analyses. To overcome these challenges, we have developed a matrix approach, which reorganizes the C balance equations in the original ESM into one matrix equation without changing any modeled C cycle processes and mechanisms. We applied the matrix approach to the Community Land Model (CLM4.5) with vertically-resolved biogeochemistry. The matrix equation exactly reproduces litter and soil organic carbon (SOC) dynamics of the standard CLM4.5 across different spatial-temporal scales. The matrix approach enables effective diagnosis of system properties such as C residence time and attribution of global change impacts to relevant processes. We illustrated, for example, the impacts of CO<sub>2</sub> fertilization on litter and SOC dynamics can be easily decomposed into the relative contributions from C input, allocation of external C into different C pools, nitrogen regulation, altered soil environmental conditions, and vertical mixing along the soil profile. In addition, the matrix tool can accelerate model spin-up, permit thorough parametric sensitivity tests, enable pool-based data assimilation, and facilitate tracking and benchmarking of model behaviors. Overall, the matrix approach can make a broad range of future modeling activities more efficient and effective.

## KEYWORDS

carbon storage, CO<sub>2</sub> fertilization, data assimilation, residence time, soil organic matter

\*Authors co-lead the research.

## 1 | INTRODUCTION

Terrestrial ecosystems absorb approximately 30% of the anthropogenic carbon dioxide (CO<sub>2</sub>) emissions, which partially

counterbalances anthropogenic CO<sub>2</sub> emission and, thus, plays an important role in mitigating future climate warming (Canadell et al., 2007). The scientific community relies strongly on global land carbon (C) models to synthesize mechanisms that regulate land-atmosphere CO<sub>2</sub> exchanges, quantify responses of land CO<sub>2</sub> fluxes to external forcing, and predict future land C-uptake strength (Ciais et al., 2013). For example, predictions of future CO<sub>2</sub> dynamics in the 5th Intergovernmental Panel on Climate Change (IPCC) report are primarily derived from global models (with the land C model as a key component) participated in the Coupled Model Intercomparison Project Phase 5 (CMIP5). Despite their importance in climate change assessment and research, global land C models possess some inherent shortcomings, such as low traceability due to their complexity, large computational resources required for spin-up, and computational costs being too high to conduct thorough sensitivity analysis (Friedlingstein et al., 2014; Lu, Wang, Ziehn, & Dai, 2013; Luo et al., 2009; Washington, Buja, & Craig, 2009). It is imperative to develop innovative approaches to make global models a more effective tool for C cycle research.

Global land C models typically represent hundreds of biophysical, biogeochemical, and ecological processes interacting with each other across different spatial-temporal timescales to mimic real world C dynamics. C dynamics can be conceptually described by a series of C balance equations, capturing C input through photosynthesis, transfers among compartments, losses through respiration and land use or disturbances. However, sophisticated behaviors arise when model structures (e.g., the number of C pools and explicitly represented processes) differ, model parameters vary, and/or initial and boundary conditions (e.g., temperature) evolve with system dynamics. Without a systematic framework, it is difficult to disentangle contributions from a specific component to the final model outputs, as each element can potentially interact with other elements of the system. The soil organic matter (SOM) decomposition rate, for example, is regulated by temporal and/or spatial varying vegetation characteristics (e.g., litter quality and rooting depth), soil thermal dynamics (e.g., soil temperature and freeze-thaw cycle), hydrological conditions (e.g., soil moisture), edaphic factors (e.g., soil texture), redox status, and nutrient levels (Luo et al., 2016). SOM decomposition, on the other hand, can potentially feed back to all of these processes through different mechanisms. In addition to being complex, global land C models are computationally expensive. Land C models, mostly due to slow soil C processes, take long time to stabilize. With a typical 1° × 1° spatial resolution, it normally takes thousands of processor hours to spin-up a model to the steady state (Washington et al., 2009), which is normally not affordable to most of the scientific community, and which becomes particularly expensive when varying parameters, such that every parameter perturbation must be equilibrated separately.

The complex nature of these global models and associated high computational costs limit our understanding of model results. For example, simulated land C fluxes in CMIP5 range from a source of 165 PgC to a sink of 758 PgC accumulated over 1,850–2,100 (Friedlingstein et al., 2014). Reasons for such a large discrepancy among models are difficult to track and the credibility from modeling are discounted. As they develop, land C models tend to incorporate

more and more processes, making them more complex. For instance, microbial activities (Wieder et al., 2015), soil C vertical profiles (Koven et al., 2013), plant species interactions (Fisher et al., 2015; Weng et al., 2015), nutrient regulations (Gerber, Hedin, Oppenheimer, Pacala, & Shevliakova, 2010; Thomas, Brookshire, & Gerber, 2015), crop dynamics (Lu, Jin, & Kueppers, 2015) and disturbances (Landry, Price, Ramankutty, Parrott, & Matthews, 2016; Shevliakova et al., 2009; Yue et al., 2014) are all considered to be important components that have been included in land models in recent years. As a result, computational requirements surge further and become a bottleneck for progress. It is almost impossible to get a full picture of the sensitivity of different C cycling processes to relevant parameters across the globe. To conduct sensitivity tests, compromises have to be made, for example, by choosing a small set instead of all relevant parameters, prescribing initial conditions instead of through spin-up, or focusing on a small local range instead of the global sensitivity.

There is a need for innovative tools to systematically tackle the efficiency and traceability challenges faced by land C models. Several model intercomparison projects (MIPs), such as CMIP5, TRENDY (<http://dgvn.ceh.ac.uk/node/9>) and MsTMIP (Huntzinger et al., 2013), were designed to diagnose, interpret and address disagreements in model performance and to track uncertainties in future C projections. These MIPs are helpful in identifying mismatches and uncertainties among models, but remain largely descriptive rather than insightful in tracing the origins of model differences. Xia, Luo, Wang, and Hararuk (2013) developed a new framework to decompose the complex model outputs into traceable components and track modeled ecosystem C storage capacity through ecosystem C input (e.g., net primary productivity, NPP), and residence time. Unfortunately, this framework is only applicable to steady state conditions. Koven, Lawrence, and Riley (2015) used a similar approach to decompose the dynamics of several CMIP5 model responses to CO<sub>2</sub>, climate, and both CO<sub>2</sub> and climate together using a 2-pool (live and dead) approximation and concluded that model dynamics of both pools to all sets of forcings are largely driven by productivity rather than turnover, which likely represents a consistent bias shared by models. Luo et al. (2017) explored transient dynamics of modeled terrestrial C in a 3-dimensional (D) parameter space, i.e., C input, residence time, and the storage potential which reflects the difference between C storage capacity and actual C storage. The 3-D parameter space provides a novel theoretical framework to evaluate and trace transient C dynamics. It can also potentially be used to understand and fundamentally improve the low traceability issue of land models. The transient dynamics analysis proposed by Luo et al. (2017) is based on matrix representation of C cycle, which has not yet been realized in global models.

To address the above limitations, we develop a matrix approach to global land C modeling. Specifically, we reorganize the 70 carbon balance equations in the Community Land Model Version 4.5 (CLM4.5) into one matrix equation to describe C transfer among organic pools in 10 soil layers. We first verify that the matrix equation fully reproduces simulation results of the original CLM4.5. Then, we demonstrate scientific and technical advantages of this matrix approach in two aspects: the calculation of diagnostic parameters,

and the attribution of the global C cycle response to CO<sub>2</sub> increases to various component processes. We also discuss additional novel applications of the matrix approach for model spin-up, traceability analysis, data assimilation, and benchmark analysis.

## 2 | MATERIALS AND METHODS

### 2.1 | CLM4.5 overview

Community Land Model Version 4.5 couples processes that regulate terrestrial energy, water, C and other biogeochemical cycles (Koven et al., 2013; Oleson et al., 2013). Specifically for biogeochemistry, CLM4.5 tracks vertically-resolved C and nitrogen (N) state variables in different vegetation, litter and SOM pools. We focus mainly on CLM4.5bgc which adopts the Century style soil C pool structure (Koven et al., 2013).

Organic matter passes from vegetation pools (leaf, root and wood) to coarse woody debris (CWD) and litter pools. CLM4.5bgc currently divides litter into three categories, corresponding to metabolic, cellulose and lignin materials (Figure 1). CWD is decomposed and respired out as CO<sub>2</sub> or gradually transferred into litter pools while decomposition of litter forms SOM. SOM is also represented by 3 categories with different turnover times. SOM is transferred among different SOM categories. In each soil layer, these transfers are regulated by transfer coefficients, fractions respired as CO<sub>2</sub>, decomposition rates and environmental (e.g., temperature, moisture and oxygen) and N conditions that regulate decomposition rates. The model tracks soil C and N dynamics up to 3.8 m depth with 10 soil layers. The same organic matter category among different vertical soil layers is allowed to mix mainly through diffusion and advection in order to represent transport processes such as bioturbation and cryoturbation through the soil profile. Detailed description of biogeochemical processes is available in Koven et al. (2013) and Oleson et al. (2013).

### 2.2 | Matrix representation

We reorganized the original model formulations into one matrix equation that captures CWD, litter and SOM dynamics. The state variables of C pools are represented by a 70 × 1 vector  $X(t)$ , i.e.,  $(X_1(t), X_2(t), X_3(t), \dots, X_{70}(t))^T$ , corresponding to seven organic C categories in each of the soil layer for 10 layers. Changes in C pool size is:

$$\frac{dX(t)}{dt} = B(t)I(t) - A\xi(t)KX(t) - V(t)X(t) \quad (1)$$

where  $B(t)I(t)$  ( $70 \times 1$ ) is the vegetation C inputs, which are distributed along the soil profile among CWD and litter pools. The second term ( $A\xi(t)KX(t)$ ) in the right side represents C dynamics within one soil layer that take into account SOM decomposition, losses through respiration and transfers among different C categories in the same soil layer. The third term ( $V(t)X(t)$ ) captures C dynamics in the vertical soil profile through different mixing mechanisms (e.g., diffusion and advection).  $t$  in parentheses indicates that the corresponding process changes with time.

$I(t)$  is the total organic C inputs while  $B(t)$  is the allocation vector ( $70 \times 1$ ).  $K$  is a  $70 \times 70$  diagonal matrix with each diagonal element representing the intrinsic decomposition rate of each C pool. In CLM4.5bgc, the intrinsic  $k$  terms are the same for all the 10 layers but differ for each type of C category, so there will be 7 unique terms in the matrix.  $K$  is modified by the scalar matrix  $\xi(t)$ , a  $70 \times 70$  diagonal matrix with each diagonal element denoting environmental and N limiting factors that regulate decomposition. Each diagonal element ( $\xi'_i$ ) of the scalar matrix combines temperature ( $\xi'_T$ ), water ( $\xi'_W$ ), oxygen ( $\xi'_O$ ), depth ( $\xi'_D$ ), and nitrogen ( $\xi'_N$ ) impacts on decomposition; of these elements in CLM4.5bgc, all but  $\xi'_N$  are the same for each pool within a given layer,

$$\xi' = \xi'_T \xi'_W \xi'_O \xi'_D \xi'_N \quad (2)$$

$A$  is the C transfer matrix ( $70 \times 70$ ) that quantifies C movement among different categories. The diagonal entries of  $A$  are ones,

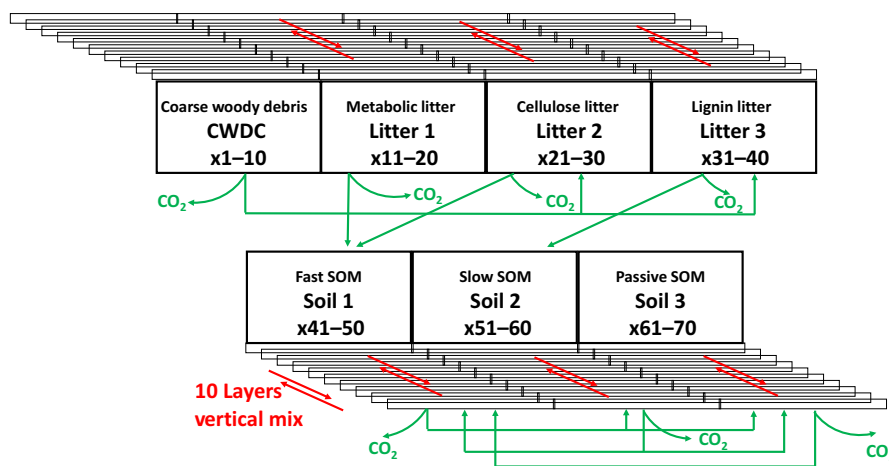


**FIGURE 1** Schema of CLM4.5bgc carbon processes on which the matrix equation (Equation 1) is based. The soil module tracks 7 carbon pool categories that are distributed into 10 soil layers, resulting in 70 pools (x1–70) in the matrix representation. soil organic matter stands for soil organic matter and coarse woody debris C (CWDC) for carbon from coarse woody debris. Red arrows indicate vertical carbon mixings which can occur in both directions: from layer  $i$  to  $i + 1$  or from layer  $i + 1$  to  $i$ . Each CWDC, Litter 1, Litter 2 and Litter 3 layer obtains carbon input from vegetation. In addition to vertical mixing, carbon can be either respired out of the system or transferred among different carbon pool categories (green arrows)

corresponding to the entire decomposition fluxes produced from each C pool. The non-diagonal entries ( $a_{ij}$ ) represent the fraction of C moving from the  $j$ th to the  $i$ th pool. For example,  $a_{42}$  indicates the fraction of C from the 2nd pool that is transferred to the 4th pool during decomposition. In this way, the  $i$ th row of the A matrix summarizes the fraction that exits and enters the  $i$ th pool. In CLM4.5bgc, transfer coefficients are set to be the same in each soil layer. The structure of A is illustrated through the block matrix,

$$A = \begin{pmatrix} A11 & 0 & 0 & 0 & 0 & 0 & 0 \\ 0 & A22 & 0 & 0 & 0 & 0 & 0 \\ A31 & 0 & A33 & 0 & 0 & 0 & 0 \\ A41 & 0 & 0 & A44 & 0 & 0 & 0 \\ 0 & A52 & A53 & 0 & A55 & A56 & A57 \\ 0 & 0 & 0 & A64 & A65 & A66 & 0 \\ 0 & 0 & 0 & 0 & A75 & A76 & A77 \end{pmatrix} \quad (3)$$

Each block entry represents a  $10 \times 10$  matrix corresponding to 10 soil layers. The diagonal block entries (A11, A22, A33, A44, A55, A66, A77) denote seven  $10 \times 10$  identical matrices, while the non-diagonal block entries (non-zeros) are  $10 \times 10$  diagonal matrices with different transfer coefficients for different matrices. Numbers correspond to seven C categories, i.e., CWD, litter1, litter2, litter3, soil1, soil2 and soil3. For example, A31 indicates the fraction of C transferred from CWD to litter2. Since the transfer coefficient ( $f_{31}$ ) is the same for different soil layers,

$$A31 = \text{diag}(-f_{31}, -f_{31}, -f_{31}, -f_{31}, -f_{31}, -f_{31}, -f_{31}, -f_{31}, -f_{31}, -f_{31}) \quad (4)$$

$V(t)$  denotes the vertical C mixing coefficient matrix,

$$V(t) = \begin{pmatrix} V11 & 0 & 0 & 0 & 0 & 0 & 0 \\ 0 & V22(t) & 0 & 0 & 0 & 0 & 0 \\ 0 & 0 & V33(t) & 0 & 0 & 0 & 0 \\ 0 & 0 & 0 & V44(t) & 0 & 0 & 0 \\ 0 & 0 & 0 & 0 & V55(t) & 0 & 0 \\ 0 & 0 & 0 & 0 & 0 & V66(t) & 0 \\ 0 & 0 & 0 & 0 & 0 & 0 & V77(t) \end{pmatrix} \quad (5)$$

Each of the diagonal block is a tridiagonal matrix (except V11) that describes mixings of the corresponding C pool category among different soil layers. CLM4.5bgc assumes no vertical mixings of CWD. Therefore, V11 is a zero matrix. As the vertical mixing rates are not differentiated among different C pool categories, V22, V33, V44, V55, V66, and V77 are identical with the following structure,

$$V22 = \text{diag}(z_1, z_2, \dots, z_{10})^{-1} \begin{pmatrix} g_1 & -g_1 & 0 & 0 & \dots & 0 & 0 & 0 \\ -h_2 & h_2 + g_2 & -g_2 & 0 & \dots & 0 & 0 & 0 \\ 0 & -h_3 & h_3 + g_3 & -g_3 & \dots & 0 & 0 & 0 \\ 0 & 0 & -h_4 & h_4 + g_4 & \dots & 0 & 0 & 0 \\ \vdots & \vdots & \vdots & \vdots & \ddots & \vdots & \vdots & \vdots \\ 0 & 0 & 0 & 0 & \dots & h_8 + g_8 & -g_8 & 0 \\ 0 & 0 & 0 & 0 & \dots & -h_9 & h_9 + g_9 & -g_9 \\ 0 & 0 & 0 & 0 & \dots & 0 & -h_{10} & h_{10} \end{pmatrix} \quad (6)$$

where the subscript numbers denote soil layers;  $g$  and  $h$  are vertical mixing rates (in unit of depth/time, e.g., m/year) of C between the

current soil layer and the upper layer and between the current and the lower layer respectively.  $z$  indicates the depth of each soil layer. In CLM4.5bgc,  $g_i = h_{i+1}$ ,  $i = 1, \dots, 9$ .

### 2.3 | Test and applications of matrix representation of CLM4.5bgc

We incorporated this matrix representation into CLM4.5bgc and ran in parallel with the original model (hereafter, the default) with the same initial conditions and forcing. To verify the matrix representation, we conducted two tests: (i) a 1,000-year simulation at a single site (Brazil, 7°S, 55°W) starting from near-zero carbon stocks; and (ii), a transient 10-year global simulation starting from spun-up 1,850 initial conditions.

According to the mathematical foundation for transient C dynamics derived in Luo et al. (2017), the behavior of most land C cycle models can be diagnosed by three parameters: C input, residence time, and storage potential. To calculate these parameters, Equation 1 can be rewritten as,

$$X(t) = (A\xi(t)K + V(t))^{-1}B(t)I(t) - (A\xi(t)K + V(t))^{-1}\frac{dX(t)}{dt} \quad (7)$$

where  $(A\xi(t)K + V(t))^{-1}B(t)I(t)$  is the C storage capacity, which quantifies the maximum amount of C a system can store at the given instantaneous environmental condition at time  $t$ . C storage capacity consists of two components: C input  $I(t)$  and residence time  $(A\xi(t)K + V(t))^{-1}B(t)$  under given C input and environmental conditions. And  $(A\xi(t)K + V(t))^{-1}\frac{dX(t)}{dt}$  is the C storage potential, i.e., the difference between the storage capacity and the actual C storage.

To obtain ecosystem-level C residence time, we extended these 70 C pools to include three vegetation pools: leaf, stem and root. We lumped the leaf transfer pool and storage pool from the original model into one leaf pool. Similarly, live and dead stem transfer pools and storage pools were treated as one stem pool, and live and dead coarse root transfer pools and storage pools, fine root transfer pool and storage pool make the root pool in the matrix representation. We ran the matrix module embedded in a global version of CLM4.5bgc and calculated the matrix diagnostics at an annual

**TABLE 1** Simulation protocol to isolate the contribution of different processes to the overall CO<sub>2</sub> fertilization response

Component	S0	S1	S2	S3	S4	S5
I	$I_0$	$I_e$	$I_e$	$I_e$	$I_e$	$I_e$
B	$B_0$	$B_0$	$B_e$	$B_e$	$B_e$	$B_e$
N	$N_0$	$N_0$	$N_0$	$N_e$	$N_e$	$N_e$
$\varepsilon$	$\varepsilon_0$	$\varepsilon_0$	$\varepsilon_0$	$\varepsilon_0$	$\varepsilon_e$	$\varepsilon_e$
V	$V_0$	$V_0$	$V_0$	$V_0$	$V_0$	$V_e$

I, total C input; B, allocation of C input; N, nitrogen status;  $\varepsilon$ , climatic conditions; and V, vertical processes. Subscript 0 denotes conditions with ambient atmospheric CO<sub>2</sub> level (280 ppm), while subscript e corresponds to elevated CO<sub>2</sub> conditions (560 ppm). Each component is plugged into the matrix representation of the CLM4.5bgc to estimate C pools under six scenarios (S0–S6).

timestep with temporal averaged matrix elements. To verify matrix diagnostics, we compared C storage capacity after 360-year matrix simulation with the steady state ecosystem C storage ( $\Delta C < 0.001\%$  of total ecosystem C) obtained from CLM4.5bgc default accelerated spin-up. We also examined a permafrost site in Alaska ( $63^{\circ}53'N$ ,  $149^{\circ}13'W$ ) to illustrate the difference between calculation of residence time from the matrix approach and the standard method by dividing carbon stocks by fluxes.

With the matrix approach, it is easy to disentangle different processes that regulate C dynamics. To illustrate such functionality, we examined the responses of dead C (CWD, litter and SOM) to  $CO_2$  fertilization. We identified that changes in total C input, allocation to different C pools, N status, environmental conditions and vertical mixing are potential processes contributing to the overall  $CO_2$  fertilization effects. We first ran the default CLM4.5bgc with 280 ppm atmospheric  $CO_2$  concentration for

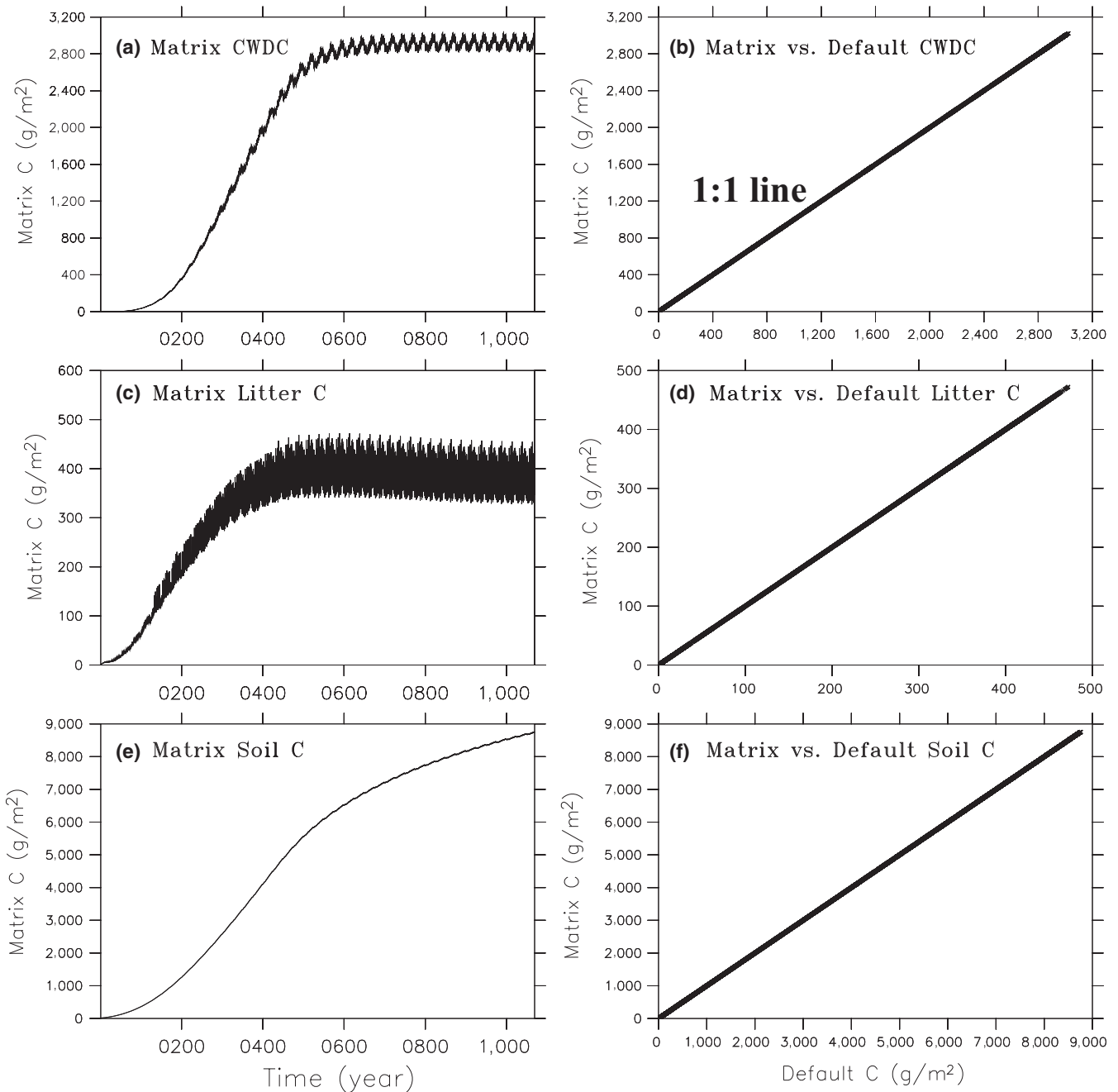


**FIGURE 2** Comparisons of dead C pools simulated from the matrix equation (Equation 1) vs. default CLM4.5bgc simulation at a Brazil site ( $7^{\circ}S$ ,  $55^{\circ}W$ ). The matrix module was run in parallel with the default CLM4.5bgc from scratch for 1,000 years. Left panels display coarse woody debris C (CWDC, a), total litter C (c) and total soil C (e) from the matrix simulation, and the right panels (b, d, f) plot corresponding simulation results from the default (x axes) vs. from the matrix module (y axes). The 1:1 lines indicate simulated C pools from the matrix module 100% match these from the default CLM4.5bgc model

10 years with initial C pools that approximate 1,850 equilibrium conditions. In a second default CLM4.5bgc simulation, everything is the same except with the 560 ppm atmospheric CO<sub>2</sub> concentration. From these two simulations, we can obtain carbon input into different litter pools (from which total carbon input and allocation coefficients can be derived, Appendix S1), N scalar, environmental scalars (e.g., soil moisture, temperature and oxygen) and active layer depth (based on which the vertical mixing rates are derived, Appendix S1) under both 280 and 560 ppm atmospheric CO<sub>2</sub>

concentrations. We fed these data into the matrix equation and conducted a series of matrix operations as illustrated by Table 1 to attribute CO<sub>2</sub> fertilization responses to process mentioned above. The baseline matrix simulation (Equation 1, Table 1, S0) was conducted with outputs of carbon inputs, N status, environmental conditions and active layer depth from the 280 ppm default CLM4.5bgc simulation. We manipulated these processes by sequentially plugging in one dataset derived from the 560 ppm default CLM4.5bgc simulation (Table 1). For example, S1 matrix

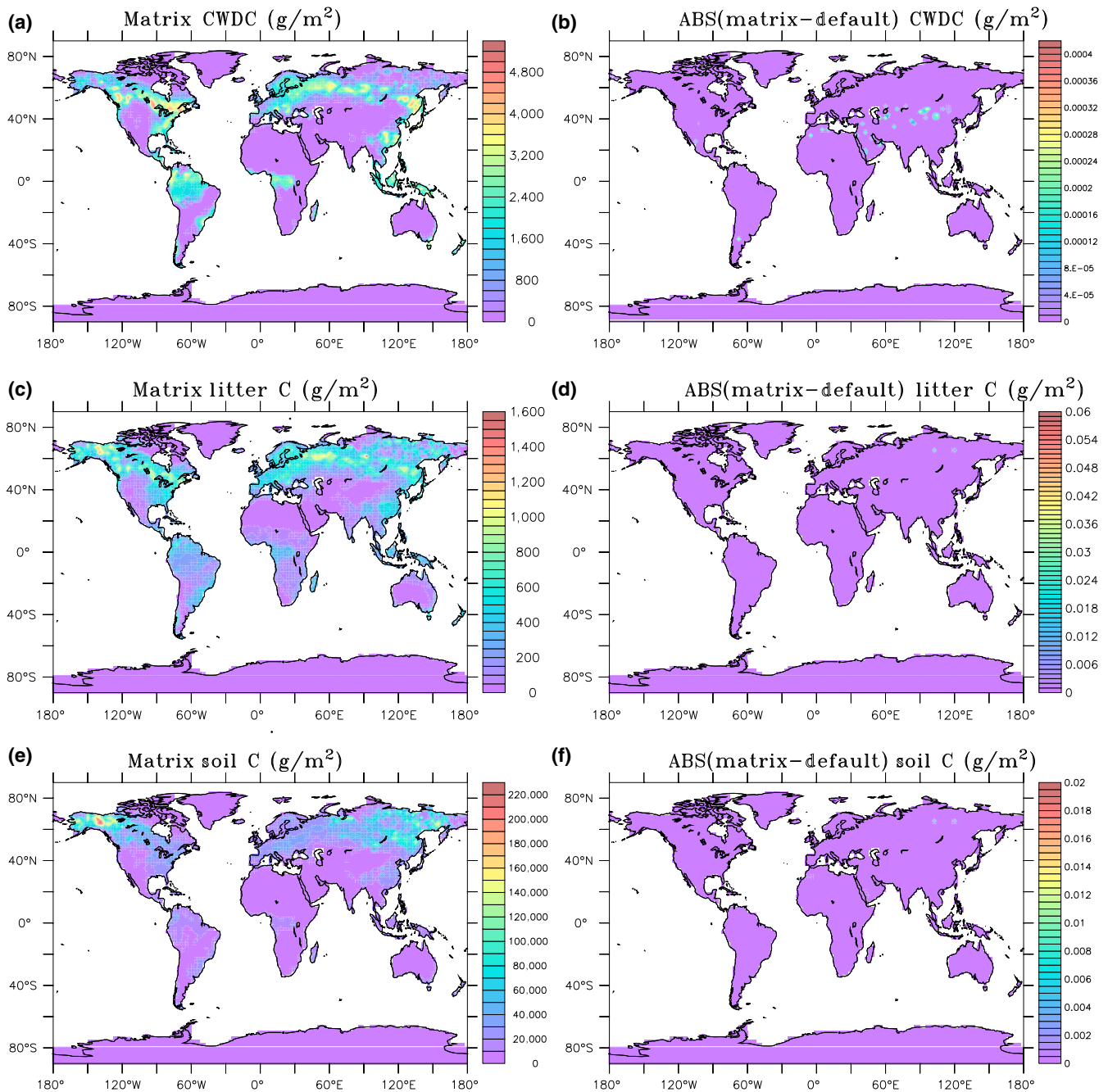


**FIGURE 3** C pools from the matrix module vs. the default CLM4.5bgc. Similarly as in Figure 2, the left three columns show simulation results from the matrix module, while the right three columns display the corresponding absolute differences between the matrix and the default CLM4.5bgc. Results are averaged over 10 years for displaying purpose

simulation was conducted with total C input from CLM4.5bgc 560 ppm and all other conditions from CLM4.5bgc 280 ppm; S2 matrix simulation was conducted with total C input and the allocation from CLM4.5bgc 560 ppm while the remaining conditions based on CLM4.5bgc 280 ppm, and so on. Therefore, the contribution of total C input is derived from the difference between S1 and S0, and the contribution of the allocation is the difference between S2 and S1 and so on.

### 3 | RESULTS AND DISCUSSION

#### 3.1 | Verification of matrix representation

The matrix model perfectly reproduces the default patterns in both long timescale single site (Figure 2) and shorter timescale global (Figure 3) simulations. At the Brazil site, C stocks accumulate with time since the run was initialized with small C stocks (Figure 2). The matrix simulation follows exactly the same pattern as the default, illustrated by the fact that points fall exactly on the 1:1 line (Figure 2). At the global scale, differences between the matrix approach and the default CLM4.5bgc simulated C pools are essentially zero (Figure 3). Simulated soil C can reach the level of 100,000 gC/m<sup>2</sup> in the northern high latitudes, while the largest difference between the matrix and the default is only around 0.02 gC/m<sup>2</sup>.

#### 3.2 | Application 1: 3D parameter space for diagnosis of the original model

Tropical regions have more C input (Figure 4a) while northern high latitudes are characterized by long C residence time (Figure 4b), both of which characteristics can lead to high C storage capacity (Figure 4c). After 360-years matrix simulation, the difference between diagnosed C storage capacity and the steady state C stock from a full default CLM4.5bgc spin-up is small, with a difference around 0.5% in global C stock estimation. The small difference is valid for most of the global grid cells despite regional variations (Figure 4d).

Starting from the near-zero initial condition, ecosystem C input, residence time, storage capacity and the actual C storage increase with time (Figure 5). The actual C storage chases C storage capacity until both reach the system steady state. When the actual C storage grows slower than C storage capacity, C storage potential increases with time and vice versa. And C storage potential stays at 0 when the system stabilizes. The rate of change in C storage is proportional to C storage potential based on the mathematical properties derived from Luo et al. (2017), and C storage potential offers an additional diagnostic on transient C dynamics.

In addition to the 3rd dimension (C storage potential) that brings novel angle in diagnosing global land C dynamics, the matrix also expands our understanding on C residence time. The common practice of dividing total C stocks by fluxes offers an easy mathematical

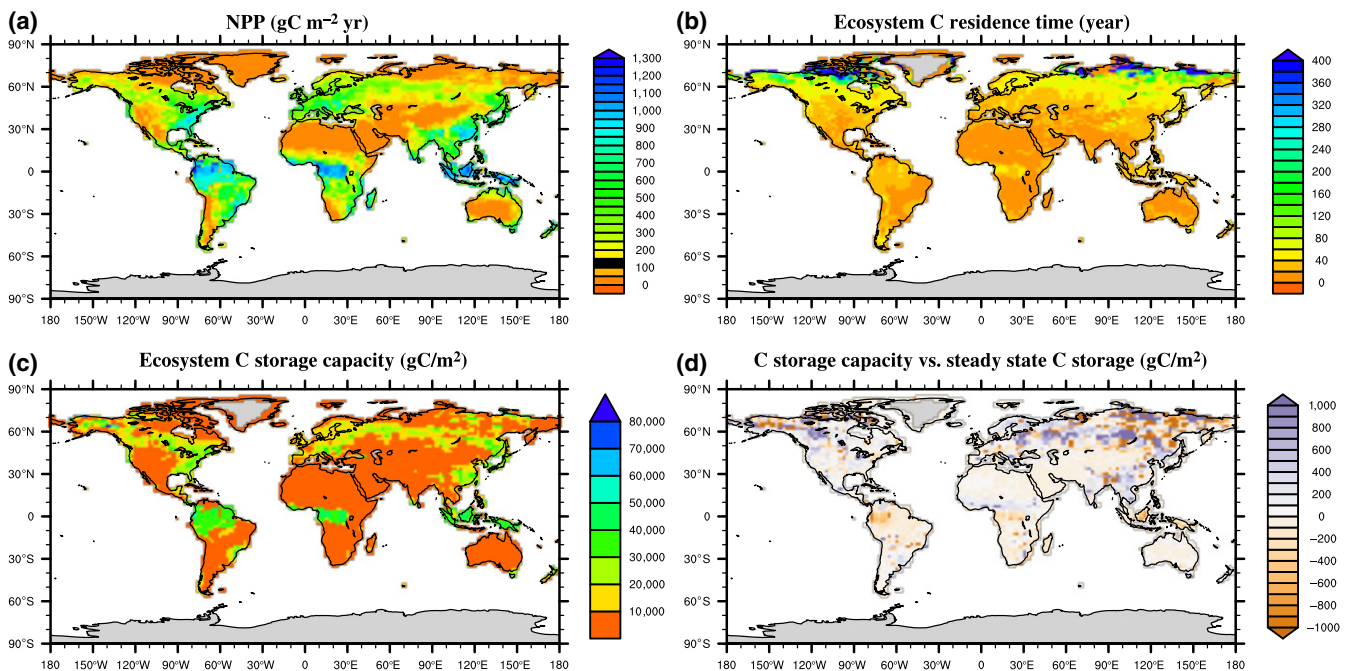


**FIGURE 4** (a) Ecosystem C input (i.e., net primary production, NPP), (b) ecosystem C residence time (transit time), and (c) ecosystem C storage capacity diagnosed from the matrix equation. (d) Difference between C storage capacity after 360 years of matrix simulation and the steady state total carbon ( $\Delta C < 0.001\%$  of total global ecosystem C) from default CLM4.5 spin-up. Model configuration is slightly different from simulations for Figure 3 with the `decomp_depth_efolding` (regulates the distribution of C input along the vertical profile) equals 10.0 instead of 0.5 in addition to the initial condition. This set-up requires less time for the default CLM4.5 to reach the steady state criterion and reduces the chances that some grid cells (especially in the northern high latitudes) are not stabilized despite the global total carbon stock stays relative stable

way to calculate how long C is likely to stay in a certain compartment and is widely applied in C cycling studies (Carvalho et al., 2014; Friend et al., 2014; Tian et al., 2015), but can be misleading especially under non-steady state condition (Sierra, Muller, Metzler, Manzoni, & Trumbore, 2016). At the Alaskan site, the matrix C residence time is relatively constant after NPP is stabilized while stock/NPP calculation still changes with time (Figure 5). In this case, after NPP stabilizes, the system can be treated as an autonomous system with constant input and decomposition rates at the annual timescale. The stock/NPP approach is validate only when the system is at steady state, but soil carbon still takes some time to reach the steady state, which makes the stock/NPP residence time deviate from that diagnosed from Equation 7. C residence time from Equation 7 provides information about system properties under given carbon input and environmental conditions, treating the system at each interested timestep as an autonomous system (constant input and decomposition rates). In addition to the case illustrated here, global land carbon models can also benefit from mathematical or theoretical advancements in tracking residence time through the non-autonomous system (with time dependent input, transfers, decomposition rates or vertical mixing rates etc.) approach, such as through the method presented by Rasmussen et al. (2016). C residence time from the matrix can be further decomposed into contributions from intrinsic properties (e.g., the decomposability of SOM)

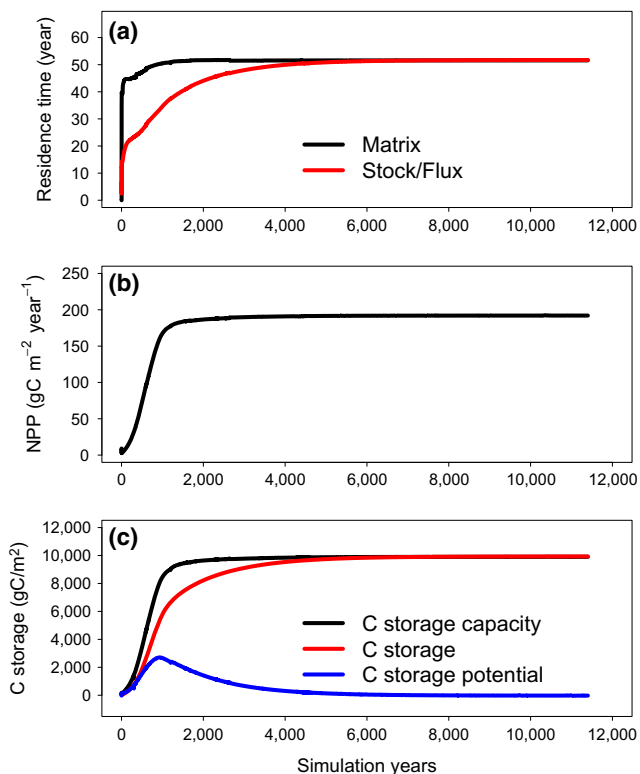


**FIGURE 5** Diagnostics of ecosystem C cycling for the Alaska (63°53'N, 149°13'W) site. (a), ecosystem C residence time diagnosed from the matrix equation (black) and C residence time calculated through dividing total C stocks by net primary production (NPP) (red). (b), ecosystem C input through NPP. (c), C storage capacity (black), actual C storage (red) and the C storage potential (blue)

and external climate regulations (Xia et al., 2013), which offers more detailed traceable information on C cycling studies.

### 3.3 | Application 2: attribution of terrestrial C response to global changes

This application is to demonstrate the effectiveness of our matrix approach to discern relative contributions of various processes to the CO<sub>2</sub> fertilization effects on litter and soil carbon dynamics. The strongest CO<sub>2</sub> fertilization impact lies in the tropical forests (Figure 6a). And the largest contribution to the overall CO<sub>2</sub> fertilization response comes from the organic C input compared to other potential factors, especially in the tropical forests (Figure 6b). In some extra-tropical regions, CO<sub>2</sub> fertilization-incurred N limitation of decomposition rates has a relatively high contribution (Figure 6d). Because of increased competition by plants under elevated CO<sub>2</sub>, the resulting N limitation reduces the decomposition rate and therefore increases C storage under elevated CO<sub>2</sub>. The contribution from altered allocation is apparent in regions such as India, Northern Australia and the non-tropical region of Africa. Altered soil environmental conditions have relatively small impacts on dead C responses to CO<sub>2</sub> fertilization in tropical regions, and have both strong positive and negative impacts in different regions across the extra-tropical regions (Figure 6e). The contribution from altered vertical mixing process is generally small and almost zero especially outside the northern high latitudes (Figure 6f).

### 3.4 | Other applications

Matrix approach makes it convenient to manipulate model components through the organized matrix to explore broad scientific questions (Ahlstrom, Xia, Arneeth, Luo, & Smith, 2015; Koven et al., 2015). Global models are generally used to quantify the overall impact of global changes on C dynamics, leaving contributions from particular processes qualitative (Ciais et al., 2013; Devaraju, Bala, Caldeira, & Nemani, 2016; Jenkinson, Adams, & Wild, 1991). In addition to attributing dead C changes in response to global changes such as CO<sub>2</sub> fertilization, warming and precipitation changes, the matrix tool is adaptable to different manipulations for exploring specific scientific questions. For example, it is relatively easy to expand the temperature scalar on soil carbon decomposition to incorporate different forms of temperature response functions (Zhou et al. under review). In this way, it is straightforward to assess how assumptions about temperature sensitivity affect large scale SOM dynamics.

The matrix approach can also boost global land C modeling efficiency through its semi-analytical solution. Despite carbon dynamics in land models are non-autonomous systems which are difficult to obtain analytical solutions (Rasmussen et al., 2016), we can still take advantage of the matrix inverse calculations to approximate system steady state and to help model spin-up. Lardy, Bellocchi, and Sousana (2011) proposed a matrix-based approach through the Gauss-Jordan elimination to effectively derive soil carbon equilibrium and is applied to shorten the spin-up of the ORCHIDEE (Naudts et al.,



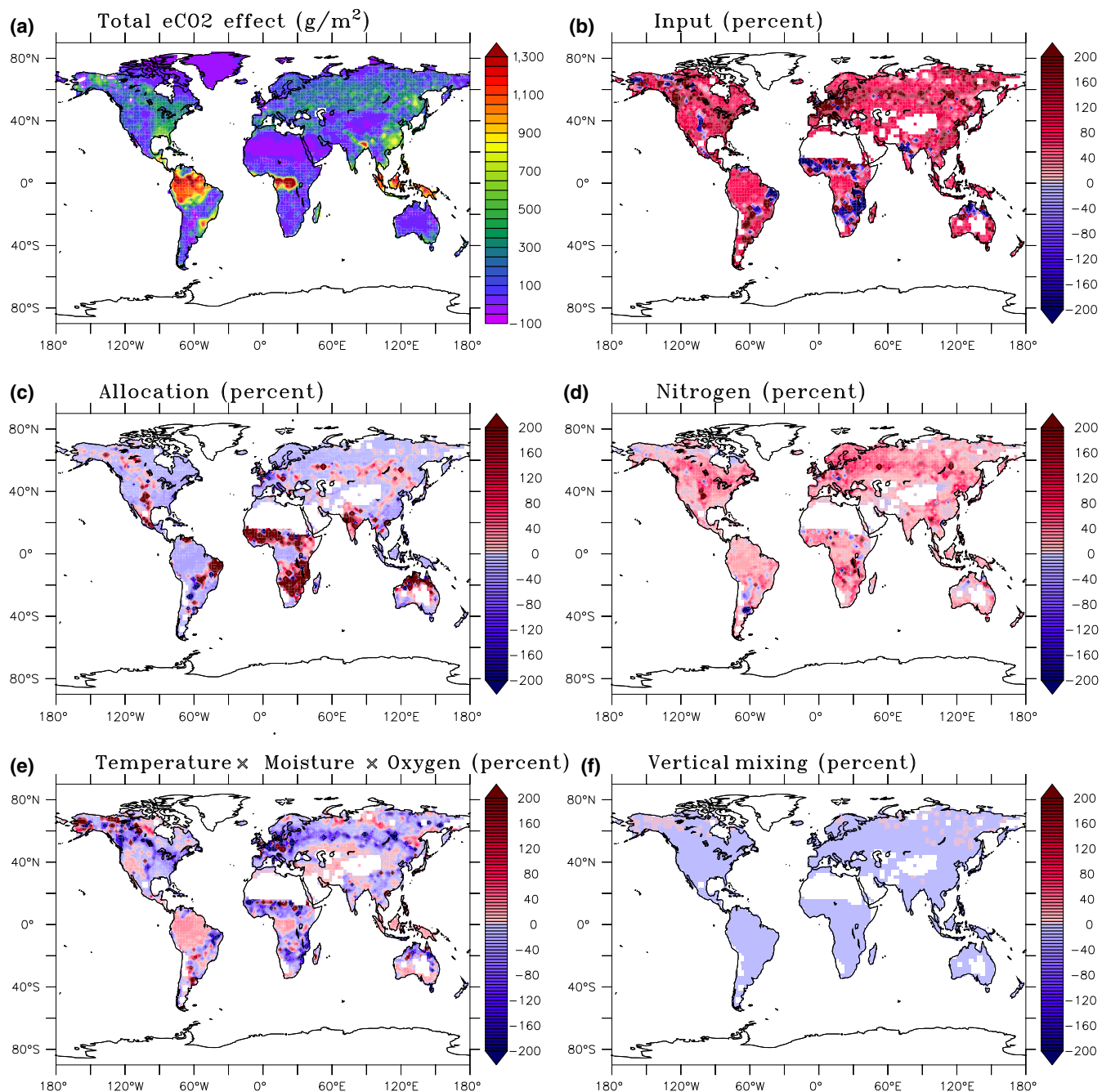


**FIGURE 6** Attribution of the total CO<sub>2</sub> fertilization effect (a) to the relative contributions from different components or processes altered by doubling of the preindustrial level atmospheric CO<sub>2</sub> (from 280 to 560 ppm). Processes that respond to CO<sub>2</sub> fertilization include: (b), total litter and coarse woody debris input; (c), allocation of the total C inputs into different C pools; (d), nitrogen status that regulates decomposition; (e), climatic and other environmental factors that scale decomposition, i.e., soil moisture, temperature, oxygen and depth; and (f), vertical mixing factors. The relative contributions are shown by percentage level (%) compared to the total CO<sub>2</sub> fertilization effect from panel (a)

2015) land surface model. Xia, Luo, Wang, Weng, and Hararuk (2012) showed that the matrix semi-analytical solution can shorten the time for spin-up of the global land C model, CABLE. Our C storage capacity after 360-years simulation is close to the quasi-steady-state obtained through default model spin-up, indicating that models with vertical soil carbon discretization can also benefit from the matrix approach. As the matrix approach semi-analytically solves soil carbon equations, it offers an efficient way to save computational resources for spin-up by one or two orders of magnitudes.

With its lower computational requirement, the matrix semi-analytical solution also enables pool-based data assimilation. The inability to assimilate C pool data has limited our ability to do global C model calibration and the matrix alleviates this constraint. For example, Hararuk, Xia, and Luo (2014) utilized the semi-analytical matrix steady state calculation to assimilate observation-based SOC pools to constrain global SOC predictions.

Furthermore, the matrix equation is generic and can be extended to incorporate more model variations as well as to other land C

models with different structures (Luo & Weng, 2011; Luo et al., 2001, 2017; Sierra & Muller, 2015). The matrix equation offers a general mathematic framework, which replicates the majority of current SOM models and allows structural flexibility that facilitates development of particular models at various levels of detail (Sierra & Muller, 2015). We showed here that the matrix approach can replicate the original land C model results even with vertically discretized soil layers. The matrix is similarly flexible in accommodating more variations, such as microbial dynamics and ecological demography modeling, simply by adding additional elements in each matrix. Divergences in modeled C pool structure are reflected in how many dimensions the matrix has and interactions among matrix elements.

With its simplicity in coding, diagnostic capability, generic structure and computational efficiency, the matrix approach can improve the efficiency of model intercomparison, benchmarking and uncertainty assessment with an ensemble of matrix equations representing the range of global land C model structures. In addition to CLM4.5 presented here, other global land models, such as CABLE (Xia et al., 2012, 2013), LPJ-GUESS (Ahlstrom et al., 2015), CLM-CASA (Hararuk et al., 2014) and CLM4.0 (Rafique et al., 2017; Wieder, Boehner, & Bonan, 2014), have showed that the matrix approach helped model-data integration, model evaluation and improvement. And matrix equations are also derived for the newly developed ORCHIDEE-MICT model (Guimberteau et al., 2017) which targets especially on the high latitude regions. Collectively, the matrix reorganizations of original models with a suite of novel matrix-based theory and tools (Luo et al., 2017; Metzler & Sierra, 2017; Rasmussen et al., 2016; Sierra et al., 2016; Xia et al., 2012, 2013) create a trackable avenue for global model-data integration, benchmark and uncertainty analyses. In addition, the matrix simulation can be conducted in one's personal computer (see Appendix S1 for an example MATLAB program that can be run at the global scale), which creates a great opportunity to explore carbon dynamics of earth system models (at least offline) especially for educators and students.

## ACKNOWLEDGEMENTS

This work was financially supported by US Department of Energy grants DE-SC0008270, DE-SC00114085, and US National Science Foundation (NSF) grants EF 1137293 and OIA-1301789.

## ORCID

Yuanyuan Huang  <http://orcid.org/0000-0003-4202-8071>

## REFERENCES

- Ahlstrom, A., Xia, J. Y., Arneeth, A., Luo, Y. Q., & Smith, B. (2015). Importance of vegetation dynamics for future terrestrial carbon cycling. *Environmental Research Letters*, *10*, 054019. <https://doi.org/10.1088/1748-9326/10/5/054019>
- Canadell, J. G., Le Quéré, C., Raupach, M. R., Field, C. B., Buitenhuis, E. T., Ciais, P., ... Marland, G. (2007). Contributions to accelerating atmospheric CO<sub>2</sub> growth from economic activity, carbon intensity, and efficiency of natural sinks. *Proceedings of the National Academy of Sciences*, *104*, 18866–18870. <https://doi.org/10.1073/pnas.0702737104>
- Carvalhois, N., Forkel, M., Khomik, M., Bellarby, J., Jung, M., Migliavacca, M., ... Reichstein, M. (2014). Global covariation of carbon turnover times with climate in terrestrial ecosystems. *Nature*, *514*, 213–217. <https://doi.org/10.1038/nature13731>
- Ciais, P., Sabine, C., Bala, G., Bopp, L., Brovkin, V., Canadell, J., ... Thornton, P. (2013). Carbon and other biogeochemical cycles. In T. F. Stocker, D. Qin, G.-K. Plattner, M. Tignor, S. K. Allen, J. Boschung, A. Nauels, Y. Xia, V. Bex & P. M. Midgley (Eds.), *Climate change 2013: The physical science basis. Contribution of working group I to the fifth assessment report of the intergovernmental panel on climate change* (pp. 465–570). Cambridge, UK and New York, NY: Cambridge University Press.
- Devaraju, N., Bala, G., Caldeira, K., & Nemani, R. (2016). A model based investigation of the relative importance of CO<sub>2</sub>-fertilization, climate warming, nitrogen deposition and land use change on the global terrestrial carbon uptake in the historical period. *Climate Dynamics*, *47*, 173–190. <https://doi.org/10.1007/s00382-015-2830-8>
- Fisher, R. A., Muszala, S., Versteinstein, M., Lawrence, P., Xu, C., McDowell, N. G., ... Bonan, G. (2015). Taking off the training wheels: The properties of a dynamic vegetation model without climate envelopes. *Geoscientific Model Development*, *8*, 3593–3619. <https://doi.org/10.5194/gmd-8-3593-2015>
- Friedlingstein, P., Meinshausen, M., Arora, V. K., Jones, C. D., Anav, A., Liddicoat, S. K., & Knutti, R. (2014). Uncertainties in CMIP5 climate projections due to carbon cycle feedbacks. *Journal of Climate*, *27*, 511–526. <https://doi.org/10.1175/JCLI-D-12-00579.1>
- Friend, A. D., Lucht, W., Rademacher, T. T., Keribin, R., Betts, R., Cadule, P., ... Woodward, F. I. (2014). Carbon residence time dominates uncertainty in terrestrial vegetation responses to future climate and atmospheric CO<sub>2</sub>. *Proceedings of the National Academy of Sciences of the United States of America*, *111*, 3280–3285. <https://doi.org/10.1073/pnas.1222477110>
- Gerber, S., Hedin, L. O., Oppenheimer, M., Pacala, S. W., & Shevliakova, E. (2010). Nitrogen cycling and feedbacks in a global dynamic land model. *Global Biogeochemical Cycles*, *24*, GB1001.
- Guimberteau, M., Zhu, D., Maignan, F., Huang, Y., Yue, C., Dantec-Nédélec, S., ... Ciais, P. (2017). ORCHIDEE-MICT (revision 4126), a land surface model for the high-latitudes: Model description and validation. *Geoscientific Model Development Discussions*, *10*, 1–65. <https://doi.org/10.5194/gmd-2017-122>
- Hararuk, O., Xia, J. Y., & Luo, Y. Q. (2014). Evaluation and improvement of a global land model against soil carbon data using a Bayesian Markov chain Monte Carlo method. *Journal of Geophysical Research-Biogeosciences*, *119*, 403–417. <https://doi.org/10.1002/2013JG002535>
- Huntzinger, D. N., Schwalm, C., Michalak, A. M., Schaefer, K., King, A. W., & Wei, Y., ... Zhu, Q. (2013). The North American carbon program multi-scale synthesis and terrestrial model intercomparison project – Part 1: Overview and experimental design. *Geoscientific Model Development*, *6*, 2121–2133. <https://doi.org/10.5194/gmd-6-2121-2013>
- Jenkinson, D. S., Adams, D. E., & Wild, A. (1991). Model estimates of CO<sub>2</sub> emissions from soil in response to global warming. *Nature*, *351*, 304–306. <https://doi.org/10.1038/351304a0>
- Koven, C. D., Lawrence, D. M., & Riley, W. J. (2015). Permafrost carbon-climate feedback is sensitive to deep soil carbon decomposability but not deep soil nitrogen dynamics. *Proceedings of the National Academy of Sciences of the United States of America*, *112*, 3752–3757. <https://doi.org/10.1073/pnas.1415123112>
- Koven, C. D., Riley, W. J., Subin, Z. M., Tang, J. Y., Torn, M. S., Collins, W. D., ... Swenson, S. C. (2013). The effect of vertically resolved soil biogeochemistry and alternate soil C and N models on C dynamics of CLM4. *Biogeosciences*, *10*, 7109–7131. <https://doi.org/10.5194/bg-10-7109-2013>

- Landry, J. S., Price, D. T., Ramankutty, N., Parrott, L., & Matthews, H. D. (2016). Implementation of a marauding insect module (MIM, version 1.0) in the integrated biosphere simulator (IBIS, version 2.6b4) dynamic vegetation-land surface model. *Geoscientific Model Development*, 9, 1243–1261. <https://doi.org/10.5194/gmd-9-1243-2016>
- Lardy, R., Bellocchi, G., & Soussana, J. F. (2011). A new method to determine soil organic carbon equilibrium. *Environmental Modelling & Software*, 26, 1759–1763. <https://doi.org/10.1016/j.envsoft.2011.05.016>
- Lu, Y. Q., Jin, J. M., & Kueppers, L. M. (2015). Crop growth and irrigation interact to influence surface fluxes in a regional climate-cropland model (WRF3.3-CLM4crop). *Climate Dynamics*, 45, 3347–3363. <https://doi.org/10.1007/s00382-015-2543-z>
- Lu, X. J., Wang, Y. P., Ziehn, T., & Dai, Y. J. (2013). An efficient method for global parameter sensitivity analysis and its applications to the Australian community land surface model (CABLE). *Agricultural and Forest Meteorology*, 182, 292–303. <https://doi.org/10.1016/j.agrfor.2013.04.003>
- Luo, Y. Q., Ahlstrom, A., Allison, S. D., Batjes, N. H., Brovkin, V., Carvalhais, N., ... Zhou, T. (2016). Toward more realistic projections of soil carbon dynamics by Earth system models. *Global Biogeochemical Cycles*, 30, 40–56. <https://doi.org/10.1002/2015GB005239>
- Luo, Y., Shi, Z., Lu, X., Xia, J., Liang, J., & Jiang, J., ... Wang, Y.-P. (2017). Transient dynamics of terrestrial carbon storage: Mathematical foundation and its applications. *Biogeosciences*, 14(1), 145–161. <https://doi.org/10.5194/bg-14-145-2017>
- Luo, Y. Q., & Weng, E. S. (2011). Dynamic disequilibrium of the terrestrial carbon cycle under global change. *Trends in Ecology & Evolution*, 26, 96–104. <https://doi.org/10.1016/j.tree.2010.11.003>
- Luo, Y. Q., Weng, E. S., Wu, X. W., Gao, C., Zhou, X. H., & Zhang, L. (2009). Parameter identifiability, constraint, and equifinality in data assimilation with ecosystem models. *Ecological Applications*, 19, 571–574. <https://doi.org/10.1890/08-0561.1>
- Luo, Y. Q., Wu, L. H., Andrews, J. A., White, L., Matamala, R., Schafer, K. V. R., & Schlesinger, W. H. (2001). Elevated CO<sub>2</sub> differentiates ecosystem carbon processes: Deconvolution analysis of Duke Forest FACE data. *Ecological Monographs*, 71, 357–376. <https://doi.org/10.2307/3100064>
- Metzler, H., & Sierra, C. A. (2017). Linear autonomous compartmental models as continuous-time Markov chains: Transit-time and age distributions. *Mathematical Geosciences*. <https://doi.org/10.1007/s11004-017-9690-1>
- Naudts, K., Ryder, J., McGrath, M. J., Otto, J., Chen, Y., Valade, A., ... Luyssaert, S. (2015). A vertically discretised canopy description for ORCHIDEE (SVN r2290) and the modifications to the energy, water and carbon fluxes. *Geoscientific Model Development*, 8, 2035–2065. <https://doi.org/10.5194/gmd-8-2035-2015>
- Oleson, K., Lawrence, D., Bonan, G., Drewniak, B., Huang, M., Koven, C., ... Thornton, P. (2013). Technical description of version 4.5 of the Community Land Model (CLM). In: *NCAR technical note NCAR/TN-503+STR* (pp. 1–420). Boulder, CO: National Center for Atmospheric Research.
- Rafique, R., Xia, J. Y., Hararuk, O., Leng, G. Y., Asrar, G., & Luo, Y. Q. (2017). Comparing the performance of three land models in global C cycle simulations: A detailed structural analysis. *Land Degradation & Development*, 28, 524–533. <https://doi.org/10.1002/ldr.2506>
- Rasmussen, M., Hastings, A., Smith, M. J., Agosto, F. B., Chen-Charpentier, B. M., Hoffman, F. M., ... Luo, Y. (2016). Transit times and mean ages for nonautonomous and autonomous compartmental systems. *Journal of Mathematical Biology*, 73, 1379–1398. <https://doi.org/10.1007/s00285-016-0990-8>
- Shevliakova, E., Pacala, S. W., Malyshev, S., Hurtt, G. C., Milly, P. C. D., Caspersen, J. P., ... Crevoisier, C. (2009). Carbon cycling under 300 years of land use change: Importance of the secondary vegetation sink. *Global Biogeochemical Cycles*, 23, GB2022. <https://doi.org/10.1029/2007gb003176>
- Sierra, C. A., & Muller, M. (2015). A general mathematical framework for representing soil organic matter dynamics. *Ecological Monographs*, 85, 505–524. <https://doi.org/10.1890/15-0361.1>
- Sierra, C. A., Muller, M., Metzler, H., Manzoni, S., & Trumbore, S. E. (2016). The muddle of ages, turnover, transit, and residence times in the carbon cycle. *Global Change Biology*, 23, 1763–1773. <https://doi.org/10.1111/gcb.13556>
- Thomas, R. Q., Brookshire, E. N. J., & Gerber, S. (2015). Nitrogen limitation on land: How can it occur in Earth system models? *Global Change Biology*, 21, 1777–1793. <https://doi.org/10.1111/gcb.12813>
- Tian, H. Q., Lu, C. Q., Yang, J., Banger, K., Huntzinger, D. N., Schwalm, C. R., ... Zeng, N. (2015). Global patterns and controls of soil organic carbon dynamics as simulated by multiple terrestrial biosphere models: Current status and future directions. *Global Biogeochemical Cycles*, 29, 775–792. <https://doi.org/10.1002/2014GB005021>
- Washington, W. M., Buja, L., & Craig, A. (2009). The computational future for climate and Earth system models: On the path to petaflop and beyond. *Philosophical Transactions of the Royal Society a-Mathematical Physical and Engineering Sciences*, 367, 833–846. <https://doi.org/10.1098/rsta.2008.0219>
- Weng, E. S., Malyshev, S., Lichstein, J. W., Farrior, C. E., Dybzinski, R., Zhang, T., ... Pacala, S. W. (2015). Scaling from individual trees to forests in an Earth system modeling framework using a mathematically tractable model of height-structured competition. *Biogeosciences*, 12, 2655–2694. <https://doi.org/10.5194/bg-12-2655-2015>
- Wieder, W. R., Allison, S. D., Davidson, E. A., Georgiou, K., Hararuk, O., He, Y., ... Xu, X. (2015). Explicitly representing soil microbial processes in Earth system models. *Global Biogeochemical Cycles*, 29, 1782–1800. <https://doi.org/10.1002/2015GB005188>
- Wieder, W. R., Boehnert, J., & Bonan, G. B. (2014). Evaluating soil biogeochemistry parameterizations in Earth system models with observations. *Global Biogeochemical Cycles*, 28, 211–222. <https://doi.org/10.1002/2013GB004665>
- Xia, J. Y., Luo, Y. Q., Wang, Y. P., & Hararuk, O. (2013). Traceable components of terrestrial carbon storage capacity in biogeochemical models. *Global Change Biology*, 19, 2104–2116. <https://doi.org/10.1111/gcb.12172>
- Xia, J. Y., Luo, Y. Q., Wang, Y. P., Weng, E. S., & Hararuk, O. (2012). A semi-analytical solution to accelerate spin-up of a coupled carbon and nitrogen land model to steady state. *Geoscientific Model Development*, 5, 1259–1271. <https://doi.org/10.5194/gmd-5-1259-2012>
- Yue, C., Ciais, P., Cadule, P., Thonicke, K., Archibald, S., Poulter, B., ... Viovy, N. (2014). Modelling the role of fires in the terrestrial carbon balance by incorporating SPITFIRE into the global vegetation model ORCHIDEE – Part 1: Simulating historical global burned area and fire regimes. *Geoscientific Model Development*, 7, 2747–2767. <https://doi.org/10.5194/gmd-7-2747-2014>

## SUPPORTING INFORMATION

Additional Supporting Information may be found online in the supporting information tab for this article.

**How to cite this article:** Huang Y, Lu X, Shi Z, et al. Matrix approach to land carbon cycle modeling: A case study with the Community Land Model. *Glob Change Biol*. 2018;24:1394–1404. <https://doi.org/10.1111/gcb.13948>